minerals

MDPI

Article

Late Cretaceous (Santonian to Campanian) Palynological Records and Paleoclimatic Significance from Borehole ZKY2-1, Songliao Basin

Zihan Zhou [1], Dangpeng Xi [1,*], Lixin Sun [2], Jing Zhao [3], Wanshu Yang [1], Yunqi Ye [1], Xinyu Meng [1] and Xiaoqiao Wan [1]

[1] State Key Laboratory of Biogeology and Environmental Geology, China University of Geosciences Beijing, Beijing 100083, China
[2] Tianjin Geological Survey Center, China Geological Survey, Tianjin 300170, China
[3] PetroChina Huabei Oilfield Company, Renqiu 062550, China
* Correspondence: xdp1121@163.com; Tel.: +86-15810903538

Abstract: The global temperature gradually decreased from the Cretaceous Santonian to Campanian, while angiosperms evolved rapidly and gradually became dominant. The Songliao Basin, NE China, contains abundant fossil palynomorphs from the Santonian to Campanian age. A thorough investigation of fossil palynomorphs in borehole ZKY2-1 of the SW Songliao Basin was performed, reconstructing the vegetation and paleoclimate transition from the Santonian–earliest Campanian (lower Nenjiang Formation) to the late Campanian (Sifangtai Formation). Eighty form-genera from borehole ZKY2-1 have been identified. Three palynomorph assemblages were identified: the *Schizaeoisporites–Cyathidites–Inaperturopollenites* assemblage, *Schizaeoisporites–Classopollis–Retitricolporites* assemblage, and *Schizaeoisporites–Aquilapollenites–Tricolporopollenits* assemblage, from bottom to top. Based on palynological analysis from ZKY2-1 and other boreholes in the Songliao Basin, angiosperm pollen proportion in the Sifangtai Formation is significantly higher than in the lower Nenjiang Formation, indicating rapid angiosperm spread from late Santonian to Campanian. Palynological records indicate relatively humid climate during this period; the content of cool palynological types increased from the lower Nenjiang Formation to the Sifangtai Formation, suggesting a transition from warm to cool climate during the late Santonian–earliest Campanian to the late Campanian. The new palynological evidence from the Songliao Basin reveals a global cooling on land and sea during the late Santonian–Campanian period. This climate change may further promote angiosperm spread during the Late Cretaceous period.

Keywords: Songliao Basin; palynomorphs; Cretaceous; Campanian; paleoclimate; vegetation

Citation: Zhou, Z.; Xi, D.; Sun, L.; Zhao, J.; Yang, W.; Ye, Y.; Meng, X.; Wan, X. Late Cretaceous (Santonian to Campanian) Palynological Records and Paleoclimatic Significance from Borehole ZKY2-1, Songliao Basin. *Minerals* **2023**, *13*, 338. https://doi.org/10.3390/min13030338

Academic Editor: Olev Vinn

Received: 5 January 2023
Revised: 21 February 2023
Accepted: 24 February 2023
Published: 27 February 2023

1. Introduction

The Cretaceous was a typical greenhouse climate period with a series of major geological events, such as large igneous provinces, the Cretaceous Normal Superchron, the Oceanic Anoxic Event, the explosion of life, and mass extinctions [1–6]. Among them, climate change from a hot greenhouse to a cool greenhouse is remarkable [1,7]. The Middle Cretaceous is a typical hot greenhouse; however, the global temperature decreased gradually during the Santonian to Campanian periods [1,7,8]. The Late Cretaceous temperature data are mainly from marine sediments [1,9,10], with only a few records coming from nonmarine Cretaceous [11,12]. Therefore, studying the terrestrial response to climatic change during the Cretaceous period is very important.

Palynology has played a significant role in reconstructing terrestrial vegetation evolution and climate during the Cretaceous period [1,13–16]. Furthermore, the palynomorphs are widely distributed during the Late Cretaceous, with angiosperm pollen

radiation [15,17–19]. Thus, palynology plays an essential role in understanding the evolution of paleoclimate and vegetation during the Late Cretaceous period.

The Songliao Basin in northeast China is one of the largest nonmarine basins worldwide, with a continuous Cretaceous terrestrial sedimentary record [20–23] (Figure 1). Microfossils such as palynomorphs, ostracods, and charophyta are abundant in the Songliao Basin [15,22,24–32]. The Cretaceous Continental Scientific Drilling borehole in the Songliao Basin (SK1) and other boreholes provide ideal materials for nonmarine Upper Cretaceous stratigraphy, paleoenvironment, and paleoclimate [12,19,21–28,33]. With the detailed study of borehole SK1 and other boreholes in the Songliao Basin, significant progress has been achieved in the chronostratigraphy of the Songliao Basin, and a high-precision year-end stratigraphic framework has been established [15,22,23,34–39]. This provides a reliable basis for studying paleoclimate, paleoenvironment, biota evolution, and major geological events in the Songliao Basin. Furthermore, the paleoclimatic characteristics of the Cretaceous in the Songliao Basin are generally studied based on the palynomorphs [17,26]. However, previous studies do not clearly state the climate change from the Santonian to Campanian periods.

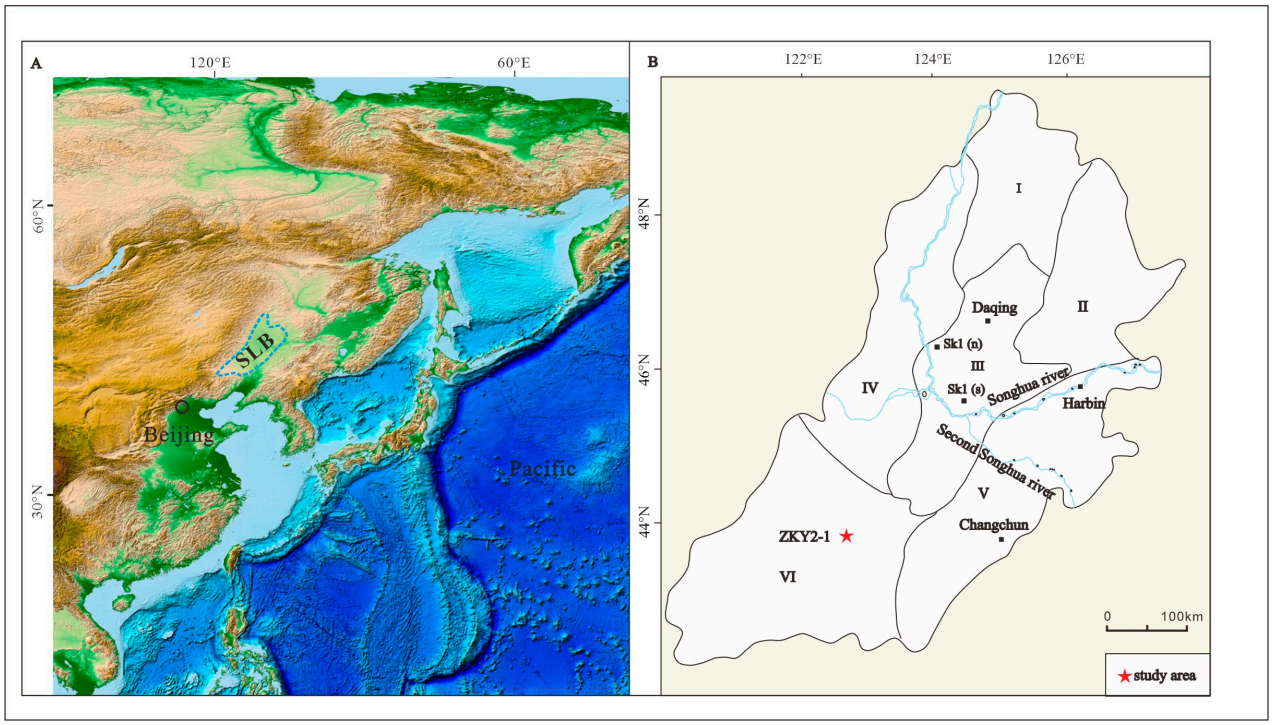

Figure 1. (**A**) Schematic diagram of Songliao Basin (SLB) and (**B**) the location of borehole ZKY2-1. I—North Plunge Zone; II—Northeast Uplift Zone; III—Central Deposition Zone; IV—West Slope Zone; V—Southeast Uplift Zone; VI—Southwest Uplift Zone.

Research concerning the Songliao Basin is mainly concentrated in the center and north, and less concentrated in the south, especially in the southwest [27]. Ostracods from the lower Nenjiang Formation (K_2n) (late Santonian to earliest Campanian) and Sifangtai Formation (K_2s) (middle to late Campanian) were recently recovered from borehole ZKY2-1 located in the SW Songliao Basin [27].

In this study, palynomorphs from borehole ZKY2-1 are investigated to establish the palynological biostratigraphy of the area, and provide the palynological data in the southwest, which makes the research data from the Songliao Basin more perfect. The study reveals the late Santonian to Campanian paleovegetation and paleoclimate significance of borehole ZKY2-1 in the southern part of the basin.

2. Geological Setting

The Songliao Basin extends from northeast to southwest, spanning the central part of Heilongjiang Province, the northeast part of Liaoning Province, the eastern part of Inner Mongolia Autonomous Region, and the western part of Jilin Province. It is about 750 km long from north to south, 370 km wide from east to west, and covers an area of about 26 km × 104 km [33] (Figure 1). The Songliao Basin has three evolution stages: a fault depression period (Huoshiling–Yingcheng Formations), a depression period (Denglouku–Nenjiang Formations), and a tectonic inversion period (Sifangtai–Yi'an Formations). The former belongs to the volcanic rift basin and the intracontinental depression basin [40]. The Songliao Basin can be divided into five first-order tectonic units: the western slope area, northern dip area, central depression area, northeast uplift area, and southwest uplift area. Borehole ZKY2-1 is located in the southwest uplift area (Figure 1). The Cretaceous sediments formed in the basin are predominantly clastic rocks. From bottom to top, the rock stratigraphic framework consists of the Huoshiling Formation (K_1h), Shahezi Formation (K_1s), Yingcheng Formation (K_1y), Denglouku Formation (K_1d), Quantou Formation (K_2q), Qingshankou Formation (K_2qn), Yaojia Formation (K_2y), Nenjiang Formation (K_2n), Sifangtai Formation (K_2s), and Mingshui Formation (K_2m) [23,41]. The Songliao Basin is rich in fossils, especially the Late Cretaceous strata [22]. The chronostratigraphic framework of the Songliao Basin has been established using magnetic, astronomical, isotopic, biostratigraphic, and quantified stratigraphic data [15,17,22,23,25,26,32,42,43] (Figure 1). K_2n is divided into five distinctive members, including K_2n^1, K_2n^2, K_2n^3, K_2n^4, and K_2n^5, from bottom to top [17]. K_2n is considered late Santonian to middle Campanian, with the Santonian/Campanian boundary at the lower K_2n^2 [22,35,36,40,44]. K_2n^1 and the lower K_2n^2 sequences mainly consist of dark gray or black mudstones and grayish to green silty mudstones intercalated with thin carbonates and deposited in deep to subdeep lake environments [30]. The upper K_2n^2 and K_2n^3, K_2n^4, and K_2n^5 consist of grayish mudstones, gray argillaceous siltstones, brownish red mudstones, and sandstones deposited in a shallow lake to delta environment [41]. K_2s comprises sedimentary facies representing riverine and lacustrine systems and other associated environments [45]. The K_2s is considered late Campanian in age [22,35,37].

With large-scale oil and gas drilling in the Songliao Basin since the 1950s, abundant fossils, especially microfossils, were discovered and accumulated. More than 20 fossil groups have been identified, of which palynomorphs are the most abundant [17,46] (Figure 2). Kong [47] summarized the main characteristics of three significant biotas: Jehol biota during the sedimentation of the Huoshiling to Shahezi Formations, the Songhuajiang biota during the depression of Yingcheng to Nenjiang Formations, and the Mingshui biota during the Sifangtai to Mingshui Formations. Gao et al. [17] summarized the palynomorph assemblages of the Late Cretaceous in the Songliao Basin, from bottom to top: 1. *Trilobosporites–Cyathidites–Tricolporopollenites* (K_2q^1-K_2q^2), 2. *Schizaeoisporites–Quantonenpollenites–Tricolporopollenites* (K_2q^3-K_2q^4), 3. *Cicatricosisporites–Cyathidites–Pinuspollenites* (K_2qn^1), 4. *Balmeisporites–Cyathidites–Classopollis* (K_2qn^2-K_2qn^3), 5. *Cyathidites–Schizaeoisporites–Tricolpites* (K_2y^1), 6. *Beaupreaidites–Cyathidites–Schizaeoisporites* (K_2y^2-K_2y^3), 7. *Proteacidites–Cyathidites–Dictyotriletes* (K_2n^1), 8. *Lythraites–Aquilapollenites–Schizaeoisporites* (K_2n^2-K_2n^5), 9. *Schizaeoisporites–Betpakdalina–Tricolporopollenites* (K_2s), 10. *Laevigatosporites–Aquilapollenites–Wodehouseia* (K_2m^1), and 11. *Tricolporopollenites–Ephedripites–Ulmoideipites* (K_2m^2). Li et al. [15] divided seven biozones from bottom to top according to the characteristics of palynomorphs in borehole SK1 (Toronian to early Danian).

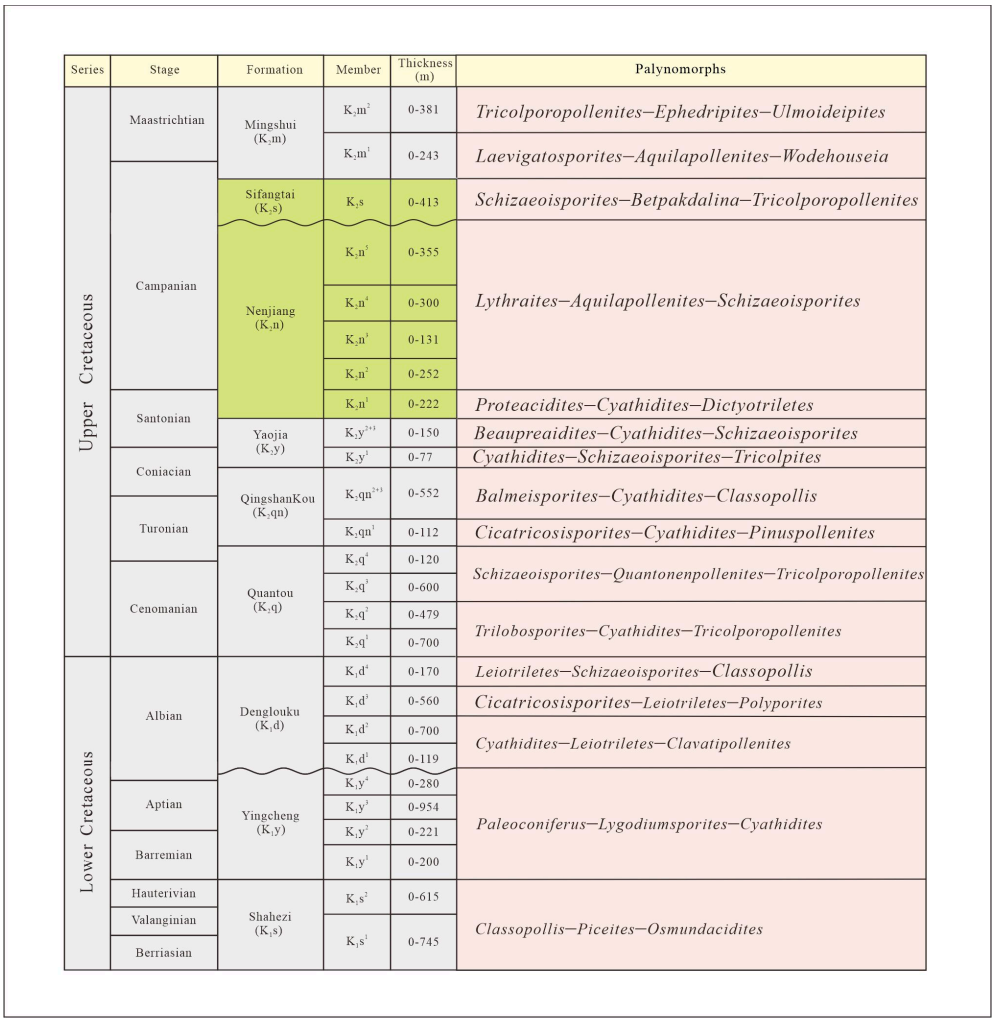

Figure 2. Cretaceous biozonation based on palynomorph assemblages in the Songliao Basin, according to [17].

3. Materials and Methods

Borehole ZKY2-1 is located in the southwestern Songliao Basin (43°56′59″ N, 122°33′45″ E), east of the Central Asia orogenic belt. The borehole is buried shallowly, and the fossils are well preserved, forming a continuous stratum from the Cretaceous Yaojia Formation to the Paleogene Taikang Formation in the southwest part of the basin. This study mainly focuses on the lower K_2n to the K_2s (240–495 m). The samples were collected at intervals of approximately 1–3 m. Twenty-five samples were selected for analysis. The lower K_2n (346–495 m) is mainly black or dark gray silty mudstone, while K_2s (240–345 m) is mainly gray-green argillaceous siltstone. All research materials are stored in the Microbiology Paleontology Laboratory of China University of Geosciences (Beijing).

Palynological analyses were performed using samples weighing 30–50 g. The samples were first treated with 10% HCl and 40% HF to remove carbonates and silicates, followed by KOH treatment to discolor organic matter. Then, KI and $ZnCl_2$ were combined into a heavy liquid (2.0 g/cm^3) that was used to separate the palynomorphs by flotation. Palynomorph identification and counting were performed at 650× magnification and, if necessary, at 800× magnification by using a Carl Zeiss microscope (Axiolab 5, Carl Zeiss AG, Oberkochen, Germany). Photos were taken using an AxioCam MRc5 digital camera (Carl Zeiss AG, Oberkochen, Germany). Considering the region's nature, palynomorph identification in this study was mainly based on relevant books [15,19,20].

CorelDRAW (2019, Corel, Ottawa, Canada) was used for drawings. The data shown were analyzed using Excel (Word Processing System 2019, Kingsoft, Beijing, China) to make line charts, and then the whole picture was drawn in CorelDRAW.

4. Results

Palynomorphs from Borehole ZKY2-1

In borehole ZKY2-1, 80 form-genera palynomorphs were preliminarily identified. (Figures 3–5, Table 1).

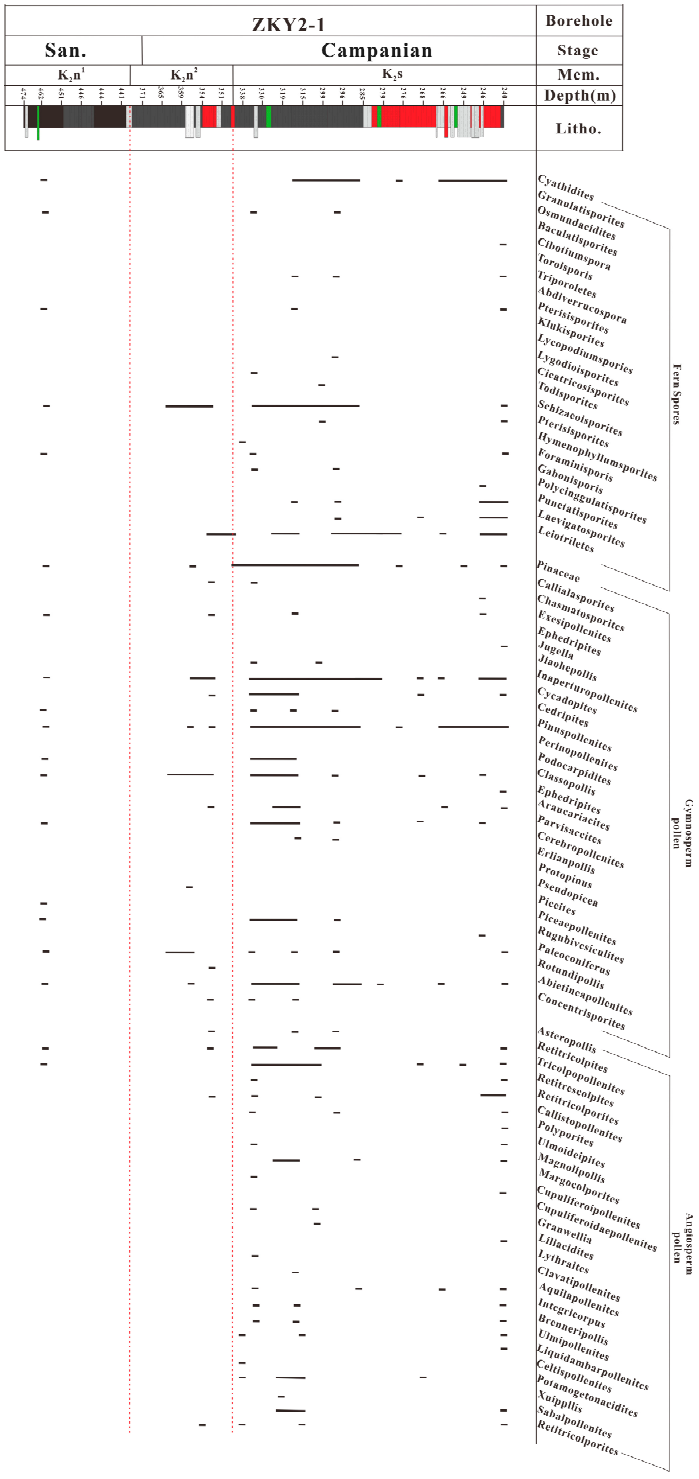

Figure 3. Distribution of the palynomorphs from K_2n^{1+2} to K_2s in borehole ZKY2-1.

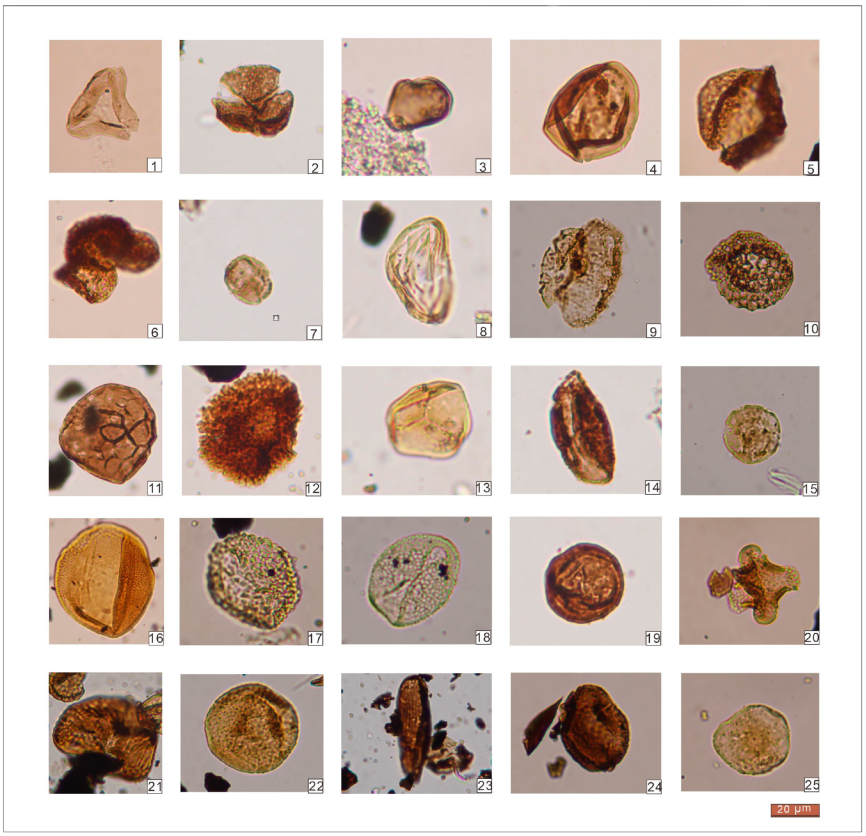

Figure 4. Typical palynomorphs from borehole ZKY2-1. 1 *Cyathidites minor*. 2 *Triphyllopollis trigonos*. 3 *Laevigatosporites*. 4 *Punctatisporites*. 5 *Piceaepollenites*. 6 *Rugubivesiculites*. 7 *Retitricolpites*. 8 *Schizaeoisporites*. 9 *Integricorpus*. 10 *Brenneripollis*. 11 *Triporoletes laevigatus*. 12 *Gabonisporites*. 13 *Todisporites minor*. 14 *Cycadopites*. 15 *Polyporites*. 16 *Paleoconiferus*. 17 *Cerebropollenites*. 18 *Liliacidites*. 19 *Classopollis classoides*. 20 *Aquilapollenites*. 21 *Cicatricosisporites*. 22 *Osmundacidites*. 23 *Jugella*. 24 *Callistopollenites*. 25 *Exesipollenites*.

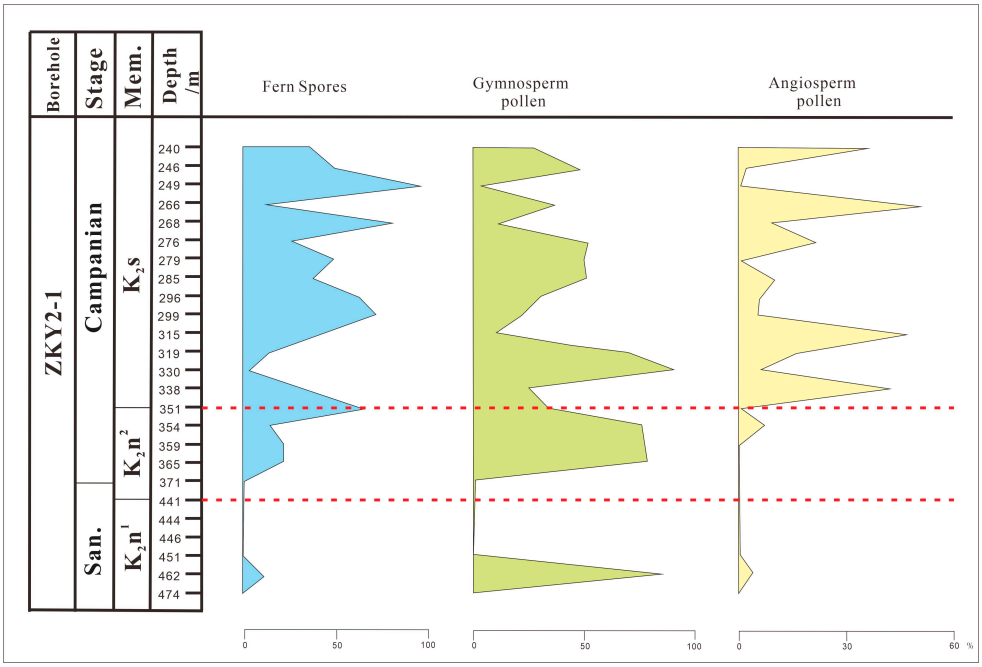

Figure 5. Variation trend in percentage of the palynomorphs from K_2n^{1+2} to K_2s in borehole ZKY2-1.

Table 1. Original data table.

		Osmundacidites	*O. wellmanii*	*Cibotiumspora*	*Todisporites*	*Pteristisporites*	*Hymenophyllumsporites*	*Salviniaspora*	*Schizaeoisporites*	*S. digitatoides*	*S. laevigataeformis*	*S. cretaceous*	*S. praeclarus*	*S. evidens*	*S. kulandyensis*	*S. sunjiawanensis*	*S. certus*	*S. applanatus*	*S. regularis*	*S. palaeocenicus*	*S. minor*	*Trilobosporites*	*Concavissmisporites*	*Lygodiumsporites*	*Lygodioisporites*	*Cicatricosisporites*	*C. minor*	*Densoisporites*	*Pteridium*	*Cyathidites*	*Cyathidites minor*	*Deltoidospora*	*Klukisporites*	*Toroisporis*	*Triporoletes*	*T. laevigatus*	*Foraminisporis*	*Biretisporites*	*Polycingulatisporites*	*Gabonisporites*	*Punctatisporites*	*Laevigatosporites*	*Leiotriletes*	Fern spores
240	K_2s			1		1		2	10	8	10	1	2	4		1	4	2			8								2	10	4			2		3				1	1	3	80
246	K_2s																												4	7	9							1		2	10	6	39
249	K_2s																												8	153	30												191
266	K_2s																																								1		1
268	K_2s																												46	24	12											2	84
276	K_2s																												1	2												3	6
279	K_2s																																									1	1
285	K_2s								6																1				3	16	5									1			32
296	K_2s								6																				18	5	7										1	2	39
299	K_2s	1			1	1			7			3	1					1				1		2				1		30	10	4			1				16	2		4	86
315	K_2s								12	3	2		2	2	1	7	2				2									4												37
319	K_2s							2	6					1									1						1	3	1		1	1						2	3	4	26
330	K_2s								2																																1		3
338	K_2s	1					2		29		5	1	1	5	1		6	1	1	1	5					1		1						1	1	2	1		1				67
351	K_2n^2																																	1								1	2
354	K_2n^2								5			2			1			1			1																					1	11
359	K_2n^2								8					1	2																											1	12
365	K_2n^2								19																																		19
371	K_2n^2																																										0
441	K_2n^1																																										0
444	K_2n^1																																										0
446	K_2n^1																																										0
451	K_2n^1																																										0
462	K_2n^1	6							10																				10	3	1	1		2		1						34
474	K_2n^1																																										0

Table 1. *Cont.*

		Podocarpidites	*P. miniusculus*	*Pinaceae*	*Pinuspollenites*	*Abietineaepollenites*	*Piceaepollenites*	*P. tobolicus*	*P. sp.*	*Cedripites*	*Laricoidites*	*Rugubivesiculites*	*Araucariacites*	*Cycadopites*	*Ephedripites*	*E. fusiformis*	*Regalipollenites*	*Jugella*	*Inaperturopollenites*	*Chasmatosporites*	*Exesipollenites*	*E. tumulus*	*Rotundipollis*	*Psophosphaera*	*Concentrisporites*	*Callialasporites*	*Jiaohepollis*	*Parvisaccites*	*Parcisporites*	*Cerebropollenites*	*Classopollis*	*C. annulatus*	*C. classoides*	*Pseudopicea*	*Piceites*	*Paleoconiferus*	**Gymnosperm pollen**
240	K_2s			4	8	2					4		5	2	2	1	4	9	19																1	61
246	K_2s	2			2							1							11	1		4	2					12			1		2				38
249	K_2s			5	1																															6
266	K_2s																		2											1							3
268	K_2s				2	4							1	2					1									1									11
276	K_2s			1	9	2																														12
279	K_2s																		1																		1
285	K_2s			11	4	11			1		2			6					4									4									43
296	K_2s			2	12	2													2																		18
299	K_2s	1		2	2	1	3			1				2														7		1	1					5	26
315	K_2s			1	3														2																		8
319	K_2s	1	2	9	29	31	3		8	1	2		8	2			1		1		1			4	1		1	25	1	1			1			2	135
330	K_2s		4	8	2	3		2	2		1		2	2					39					1				2			1						69
338	K_2s		2	6	2	3	1			1	2	1		2			1		14						1	1	1	6			1					1	46
351	K_2n^2			1																																	1
354	K_2n^2												1	3					6			3	2			1	1				2	3	7				57
359	K_2n^2			2	4	1													1												5	20	6	1		1	41
365	K_2n^2																														21	33	2			12	68
371	K_2n^2																																				0
441	K_2n^1																																				0
444	K_2n^1																																				0
446	K_2n^1																																				0
451	K_2n^1																																				0
462	K_2n^12			28	48	20	20		2	4	11	1							40		8	8		2				14	2			6	18		3	4	271
474	K_2n^1																																				0

Table 1. *Cont.*

		Cupulíferoipollenites	*Cupulíferoidaepollenites*	*Ulmoideipites*	*Ulmipollenites*	*Liquidambarpollenites*	*Celtispollenites*	*Magnolipollis*	*Liliacidites*	*Margocolporites*	*Potamogetonacidites*	*Granwellia*	*Callistopollenites*	*Asteropollis*	*Clavatipollenites*	*Aquilapollenites*	*A. minor*	*A. spinulosus*	*Lythraites*	*Integricorpus*	*Xuipplis*	*Brenneripollis*	*Polyporites*	*Sabalpollenites*	*Triphyllopollis trigonos*	*Retitrescolpites*	*Retitricolpites*	*Tricolpopollenites*	*T. mollis*	*Retitricolporites*	**Angiosperm pollen**
240	K_2s	1		3	4	2		4	4				4			4				6		6	2	3	3	4	12	6		5	77
246	K_2s																										1				1
249	K_2s																											1			1
266	K_2s																														4
268	K_2s										1						1											7			9
276	K_2s																											5			5
279	K_2s																														
285	K_2s		1					1								1											3	2			8
296	K_2s							2								1															3
299	K_2s												2	2													2				6
315	K_2s		3		5						2	1	6											2			4	10		6	39
319	K_2s							2			11			1	1					3	2	2	2	1				5			30
330	K_2s							1																			1	2			4
338	K_2s		1	1	7		1		4	1	1		23			1	2	1	1	2		2	3			2	4	5	4	15	83
351	K_2n^2																														0
354	K_2n^2													1											1		2			2	6
359	K_2n^2																														0
365	K_2n^2																														0
371	K_2n^2																														0
441	K_2n^1																														0
444	K_2n^1																														0
446	K_2n^1																														0
451	K_2n^1																														0
462	K_2n^1												2														2	6			11
474	K_2n^1																														0

In K_2n^1, there were 26 form-genera. Fern spores belonged to *Cyathidites*, *Klukisporites*, *Triporoletes*, *Foraminisporis*, *Osmundacidites*, and *Schizaeoisporites*, among others. The following gymnosperm pollen taxa were also identified: *Podocarpidites*, *Pinuspollenites*, *Abietineaepollenites*, *Piceaepollenites*, *Cedripites*, *Inaperturopollenites*, *Classopollis*, and *Pinaceae*, among others. The angiosperm pollen primarily belonged to *Callistopollenites*, *Retitricolpites*, and *Ricolpopollenites*, among others.

In K_2n^2, there are 20 form-genera. The fern spores belonged to *Triporoletes*, *Schizaeoisporites*, and *Laevigatosporites*. Among the gymnosperm pollen taxa identified were *Pinuspollenites*, *Abietineaepollenites*, *Pinaceae*, *Inaperturopollenites*, and *Classopollis*. The angiosperm pollen primarily belonged to *Asteropollis*, *Triphyllopollis*, *Tricolpopollenites*, and *Retitricolpites*.

Seventy-seven form-genera were identified in K_2s. Fern spores belonged to *Cyathidites*, *Trilobosporites*, *Abdiverrucospora*, *Osmundacidites*, *Gabonisporites*, and *Schizaeoisporites*, among others. *Podocarpidites*, *Inaperturopollenites*, *Araucariacites*, *Pinaceae*, *Jugella*, *Cycadopites*, and *Classopollis* were among the identified gymnosperms. The angiosperm pollen primarily belonged to *Callistopollenites*, *Ulmoideipites*, *Retitrescolpites*, *Asteropollis*, *Polyporites*, *Tricolpopollenites*, *Aquilapollenites*, and *Retitricolpites*, among others.

Three assemblages are divided by identification and analysis of palynomorphs of the index taxa.

K_2n^1 is represented by the *Schizaeoisporites–Cyathidites–Inaperturopollenites* assemblage. The frequency of gymnosperm pollen is high (0%–85.7%), followed by fern spores (0%–10.7%), and angiosperm pollen (0%–3.6%). Among the fern spores, *Cyathidites* are dominant (0%–38.2%), and *Schizaeoisporites* have a large concentration (0%–29.4%); *Osmundacidites* are common. Among the gymnosperm pollen are *Pinuspollenites*, *Abietineaepollenites*, and *Classopollis*. The percentage of *Inaperturopollenites* is relatively high (0%–27.6%), while *Pinuspollenites* (0%–17.7%), *Abietineaepollenites* (0%–7.3%), *Piceaepollenites* (0%–7.3%), and *Classopollis* (0%–8.7%) all have a certain amount. Among the angiosperm pollen, *Tricolpopollenites* (0%–54.5%) have a certain amount, while *Retitricolpites* and *Callistopollenites* are common.

The *Schizaeoisporites–Classopollis–Retitricolporites* assemblage belongs to K_2n^2. Gymnosperm pollen is most abundant (33.3%–78.1%), followed by fern spores (14.8%–66.6%), and angiosperm pollen (0%–8.2%). *Schizaeoisporites* are dominant (0%–100%) among the fern spores. Among the pollen of gymnosperms, including *Paleoconiferus*, *Classopollis*, and *Inaperturopollenites*, *Classopollis* possesses a larger percentage (21.1%–82.3%), while *Paleoconiferus* and *Callialasporites* are common. The angiosperm pollen, including *Asteropollis*, *Retitricolpites*, *Retitricolporites*, *Triphyllopollis*, and *Retitricolporites* (0%–33.3%), have a certain amount.

The *Schizaeoisporites–Aquilapollenites–Tricolporopollenits* assemblage belongs to K_2s, which is dominated by fern spores (3.9%–96.4%), followed by gymnosperm pollen (3%–90.7%), and angiosperm pollen (0.6%–46.5%). Among the fern spores, including *Schizaeoisporites*, *Cyathidites*, *Pterisisporites*, and others, *Cyathidites* (10.8%–84.2%) predominates, while *Schizaeoisporites* and *Gabonisporites* are common. Among the gymnosperm pollen, including *Classopollis*, *Araucariacites*, *Pinuspollenites*, and others, *Pinuspollenites* (2.8%–75%) are dominant, whereas *Classopollis* and *Araucariacites* are common. Finally, among the angiosperm pollen, *Callistopollenites*, *Tricolpopollenites* (6–77.8%), and *Retitricolporites* (6.4%–33.3%) have the highest content, while *Callistopollenites*, *Asteropollis*, and others are common.

5. Discussion

5.1. Stratigraphic Correlation between Boreholes ZKY2-1 and SK1

The Late Cretaceous integrated stratigraphic framework has been established based on borehole SK1 [22,23,36,37,39]. Therefore, comparing other boreholes and borehole SK1 is very important (Figure 6). A large-scale lake invasion occurred during sedimentation of the lower K_2n^1 and lower K_2n^2, depositing two sets of black mudstone, shale, and

oil shale [48,49]. The bottom of both K_2n^1 and K_2n^2 in boreholes SK1 and ZKY2-1 are mainly characterized by black shale and mudstone. Thus, the boundary of K_2y/K_2n^1 and K_2n^1/K_2n^1 can be easily recognized [50]. Owing to tectonic uplift, there is a widespread stratigraphic hiatus between K_2n and K_2s [51]. From K_2n to K_2s of borehole SK1, there may be 3.8 myr of stratigraphic hiatus [38]. In borehole ZKY2-1, the stratigraphic hiatus is much longer than that of borehole SK1 because there are no K_2n^3 to K_2n^5 strata [27]. K_2s is composed of dark gray, gray mudstone, and grayish green, light gray siltstone [52]. Borehole SK1 mainly revealed greenish gray mudstone and silty mudstone, light gray fine sandstone and siltstone, and grayish brown silty mudstone [53]. ZKY2-1 revealed mainly gray and dark gray mudstone, siltstone, fine sandstone, and medium sandstone, similar to borehole SK1.

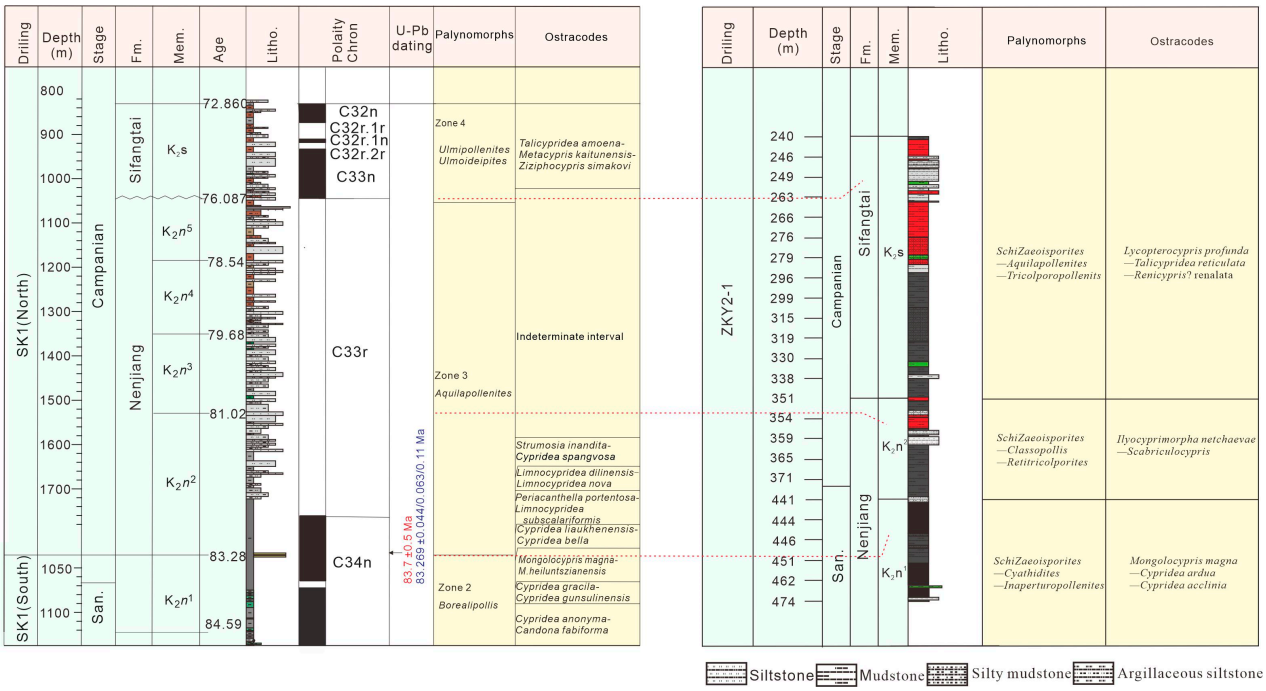

Figure 6. Stratigraphic correlation between borehole ZKY2-1 and borehole SK1. SK1 data are from reference [23].

Palynomorphs and ostracods play an important role in biostratigraphic correlation in the Songliao Basin. In borehole ZKY2-1, K_2n^1 is represented by the *Schizaeoisporites–Cyathidites–Inaperturopollenites* assemblage, with gymnosperm pollen predominating. High concentrations of *Cyathidites* and *Schizaeoisporites* are found in the fern spores, while *Osmundacidites* were found to a lesser level. *Pinuspollenites* dominate in the gymnosperm pollen, while *Pinaceae* and *Classopollis* have varying content levels. *Tricolpopollenites* from angiosperm pollen were found. In borehole SK1 [24], *Schizaeoisporites* were predominant in the fern spores, while *Cyathidites* and *Osmundacidites* were found in varying proportions. The gymnosperms pollen was abundant in *Pinaceae*, *Classopollis*, and *Pinuspollenites*. The abundance of *Tricolpopollenites* distinguishes angiosperm pollen. Generally, the palynomorph assemblage of K_2n^1 in borehole ZKY2-1 is similar to that in borehole SK1. A simple comparison was made between borehole ZKY2-1 and borehole SK1. In borehole SK1, K_2n^1 is represented by the *Cypridea gracila–Cypridea gunsulinensis* assemblage [30]. In borehole ZKY2-1, K_2n^1 is represented by the *Mongolocypris magna–Cypridea ardua–Cypridea acclinia* assemblage [27]. The two are very similar and comparable.

In borehole ZKY2-1, the lower K_2n^2 is represented by the *Schizaeoisporites–Classopollis–Retitricolporites* assemblage. The fern spore *Schizaeoisporites* predominates. Gymnosperm pollen contains a significant content of *Classopollis*. Angiosperm pollen, such as *Asteropollis*,

Retitricolpites, and *Retitricolporites*, are present in certain amounts. The abundance and diversity of palynomorphs increased gradually from bottom to top. In borehole SK1, the palynomorph assemblage of the lower K_2n^2 is represented by the *Lythraites–Callistipollehites–Schizaeoisporites* assemblage [24], with fern spores of *Schizaeoisporites* predominating in K_2n^2. The content of *Classopollis* is high in gymnosperm pollen, and three colpi characterize angiosperm pollen. The number and species of palynomorphs gradually increase from K_2n^1 to K_2n^2. Generally, the palynomorph assemblage of K_2n^2 in borehole ZKY2-1 is similar to that of borehole SK1. A simple comparison was made between borehole ZKY2-1 and borehole SK1. In borehole SK1, K_2n^2 is represented by the *Mongolocypris magna–Mongolocypris heiluntszianensis* assemblage [30]. In borehole ZKY2-1, the lower K_2n^2 is represented by *Ilyocyprimorpha netchaevae–Scabriculocypris trapezoids* [27]. It is suggested that the ostracod assemblage of the two boreholes is similar. Compared with borehole SK1, the ostracod and palynomorphs from the upper K_2n^2 to K_2n^5 are not identified.

In borehole ZKY2-1, the palynomorph assemblage of K_2s belongs to the *Schizaeoisporites–Aquilapollenites–Tricolporopollenits* assemblage. *Cyathidites* is dominant in the fern spores, *Schizaeoisporites* and *Gabonisporites* are common. *Pinuspollenites* and *Inaperturopollenites* are high in gymnosperms pollen; *Classopollis* and *Araucariacites* are common. *Tricolpopollenites* and *Retitricolporites* are high in angiosperm pollen; *Callistopollenites* and *Asteropollis* are common. In borehole SK1 [43], the fossil palynomorphs in the K_2s assemblage are dominated by gymnosperm pollen, followed by fern spores and angiosperm pollen. Generally, the palynomorph assemblage of K_2s in borehole ZKY2-1 is similar to that of borehole SK1. A simple comparison is made between borehole ZKY2-1 and borehole SK1. In borehole SK1, K_2s is represented by the *Talicypridea amoena–Metacypriskaitunensis–Ziziphocyprissimakovi* assemblage [30]. In borehole ZKY2-1, K_2s is represented by the *Lycopterocypris profunda–Talicypridea reticulata–Renicypris? Renalata* [27]. The ostracod is very similar and comparable.

The widespread distribution of *Schizaeoisporites* is an important characteristic of the Late Cretaceous palynomorph assemblage [26]. Nichols and Sweet [54] regarded the triporate type as an indication of the age of Santonian. *Callistopollenites* are common in Late Cretaceous palynomorph assemblages in the Northern Hemisphere (e.g., in the Edmonton Formation, Alberta, Canada) [55]; Li et al. [15] regarded *Callistopollenites* as late Santonian to Campanian. *Rugubivesiculites* are often found in the Campanian [18]. In the Lower Cretaceous sediments of Spain [56] and Sweden [55], *Appendicisporites* may have survived up to the Santonian period [57]. According to Nichols and Jacobson [57], *Aquilapollenites* first appeared during the Campanian. In contrast, according to Nichols and Sweet [54], *Aquilapollenites* originated during the Santonian–Campanian. The Aquliapollen type created by Gao and others in 1976 includes *Aquilapollenites*, which are widely distributed globally and mainly concentrated in Asia, North America, and in Europe north of 35° N. *Aquilapollenites* have also been found in central Africa, Malaysia, and Australia. In the Late Cretaceous, the Aquliapollen type was reported in the Rocky Mountains of the United States, Alaska, and the lower reaches of the Mississippi River; and Canada, Siberia, Japan, France and the United Kingdom; It is mainly found in the Songliao Basin, Sanjiang Basin, and Jiayin Region of Heilongjiang Province in northeast China [17]. The palynomorphs in borehole ZKY2-1 have typical characteristics of the Late Cretaceous.

By comparing borehole ZKY2-1 with borehole SK1 and analyzing the age of the palynomorph assemblages, K_2n^1 in borehole ZKY2-1 is dated as late Santonian, K_2n^2 is determined as the latest Santonian–earliest Campanian, the period of K_2s is assigned as late Campanian. The age of the lower Nenjiang Formation to Sifangtai Formation of borehole ZKY2-1 lasted from late Santonian to late Campanian, but the middle Campanian strata are missing. The established chronostratigraphic framework provides the basis for the following vegetation analysis and climate change.

5.2. Vegetation Change during the Santonian–Campanian Period

The Cretaceous period was critical for the origin and spread of angiosperms [58,59]. Although angiosperms may have appeared for a long time [60], angiosperm pollen is diffi-

cult to identify until after deposition of the Barremian strata [19]. The late Early Cretaceous epoch is considered significant for the early distribution of angiosperm pollen; nevertheless, the number and diversity are still relatively limited [17,58,61]. Angiosperms proliferated and flourished rapidly, replacing gymnosperms as the dominant group gradually during the Late Cretaceous. In the Late Cretaceous, the Santonian–Lower Campanian period was crucial for rapid angiosperm proliferation [14]. Based on the data from borehole ZKY2-1 and other boreholes/outcrops in the Songliao Basin, the rapid radiation process of angiosperms is described in detail.

Coniferous forest, evergreen broadleaf forest, deciduous broadleaf forest, shrub, and herb are the classification of palynomorphs vegetation types [17].

According to the palynomorph assemblage reaction of the late Santonian–Campanian period in borehole ZKY2-1, the K_2n^{1+2} record comprises high amounts of coniferous forest and some content of herb. Coniferous forest and herb are the dominant vegetation types. As herb content increases, coniferous and evergreen broadleaf forests have some content throughout the sedimentation of the K_2s. The vegetation types were herb and broadleaf mixed forest during this period. A comparison analysis between K_2n^{1+2} and K_2s reveals that from late Santonian–earliest Campanian to late Campanian, the vegetation type of NE Asia changed from coniferous forest and herb to herb and herb–broadleaf mixed forest (Figure 7, Table 2).

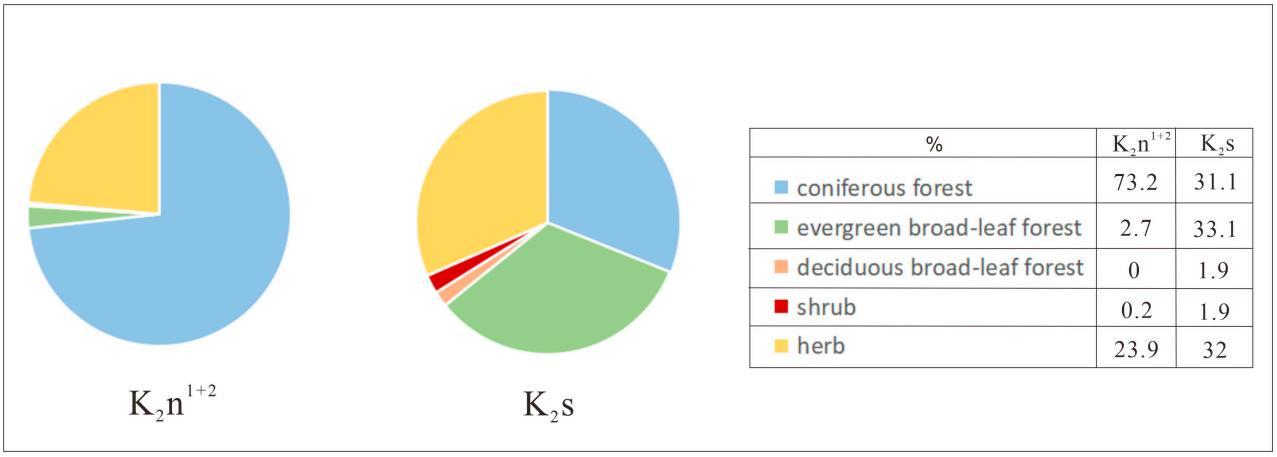

Figure 7. Ratio of different vegetation types represented by palynomorphs in borehole ZKY2-1.

Table 2. Vegetation-types table. References: (1): [17].

Vegetation Types				
Coniferous Forest	**Evergreen Broadfeaf Forest**	**Deciduous Broadleaf Forest**	**Shrub**	**Herb**
Classopollis	*Cyathidites*	*Ulmoideipites*	*Concavissimisporites*	*Laevigatosporites*
Podocarpidites	*Cibotiumspora*	*Liquidambarpollenites*	*Klukisporites*	*Schizaeoisporites*
Cedripites	*Cycadopites*	*Ulmipollenites*	*Lygodiumsporites*	*Deltoidospora*
Piceaepollenites	*Magnolipollis*		*Lygodioisporites*	*Osmundacidites*
Abietspollenites			*Aquilapollenites*	*Todisporites*
Pinuspollenites			*Integricorpus*	*Densoisporites*
Araucariacites				*Polyporites*
Parvisaccites				*Lythraites*
Palaeoconiferus				*Cicatricosisporites*
Piceites				*Ephedripites*
Inaperturopollenites				
Psophosphaera				

Late Santonian to early Campanian angiosperm pollen *Callistopollenites*, *Retitricolpites*, *Tricolpopollenites*, *Asteropollis*, and *Triphyllopollis* are found in K_2n^1 and K_2n^2 of borehole ZKY2-1. In K_2n^{1+2} of borehole ZKY2-1, the content of angiosperm pollen is very low (0%–4.4%). Considering that the number of K_2n^{1+2} in borehole ZKY2-1 is small and there may be errors, we compare and comprehensively analyze the palynomorph data for K_2n^1 and lower K_2n^2 in the Houjingou section with Yan Jingjing, and show the average proportion of angiosperm pollen (0%–12.3%) [42]. In contrast, during the middle and late Campanian periods, angiosperm pollen *Aquilapollenites* are found in K_2s of borehole ZKY2-1. In K_2s of borehole ZKY2-1, the content of angiosperm pollen increases significantly (0.5%–46.4%). The number and abundance of angiosperm pollen increases significantly from K_2n^{1+2} to K_2s (Figure 8), among which *Tricolpopollenites* and *Retitricolporites* flourished gradually, and *Aquilapollenites* appeared in K_2s. The angiosperm pollen also increased rapidly in the Songliao Basin and Jiayin Basin (NE China) from Santonian to late Campanian, [15,26,43,62,63]. In summary, in East Asia, angiosperm pollen experienced rapid radiation from late Santonian to late Campanian.

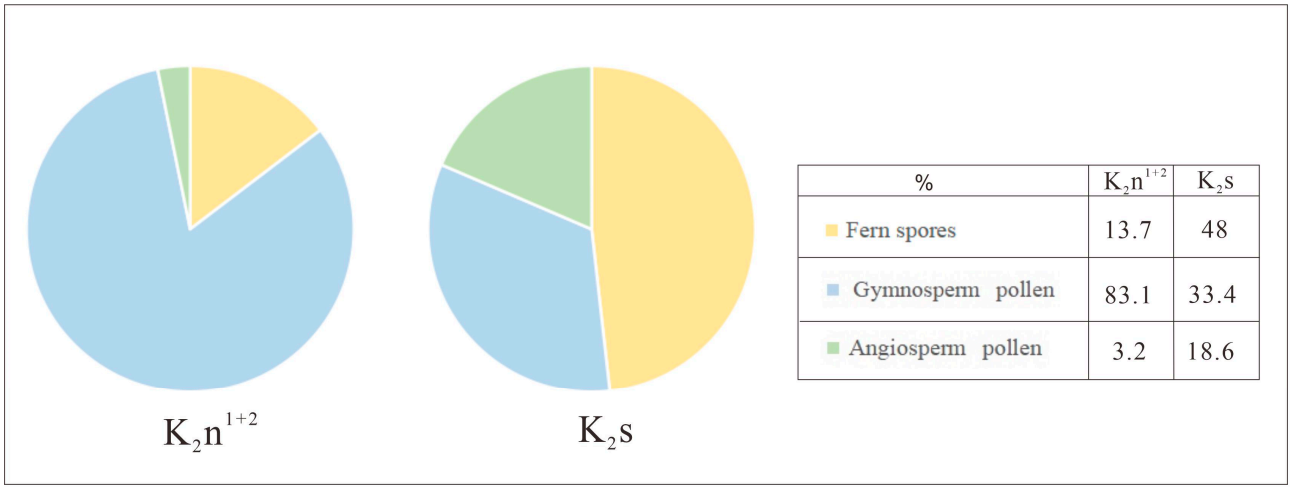

%	K_2n^{1+2}	K_2s
Fern spores	13.7	48
Gymnosperm pollen	83.1	33.4
Angiosperm pollen	3.2	18.6

Figure 8. Ratio of different types of palynomorphs in borehole ZKY2-1.

5.3. Climate Change during the Late Santonian–Campanian Period

Palynomorphs are abundant in the Songliao Basin, which can reflect the nonmarine Cretaceous paleoclimate, especially the paleoclimatic of East Asia [17,26,43]. The palynomorphs from borehole ZKY2-1 reveal minimal humidity change from K_2n^{1+2} to K_2s (or the early Santonian to late Campanian). However, there is an obvious drop in temperature from K_2n^{1+2} to K_2s.

Classopollis thrives in an arid and hot environment [64–66]. The content of *Classopollis* decreased from K_2n^{1+2} to K_2s. *Pinaceae* was the most common in semiarid- to subhumid-type climate [67–70] in borehole ZKY2-1. *Abietineaepollenites* and *Pinuspollenites* were dominant in the semiarid-type climate [68,69]. From K_2n^{1+2} to K_2s, the contents of semiarid–semihumid, semiarid, and semihumid components are relatively stable. The *Ephedripites*, representing a dry climate, are very low in both K_2n^{1+2} and K_2s, suggesting the climate was not very arid. Briefly, the dry and humid conditions during the late Santonian to Campanian periods are mainly semiarid–semihumid, with fluctuations from arid to humid. However, further study of humidity is needed in the future.

The palynomorphs from borehole ZKY2-1 can indicate the temperature of climate, and among them are hot-type Cheirolepidiaceae (*Classopollis*); warm-type Bryophyta (*Foraminisporis*), Osmundaceae (*Osmunacidites*), Araucariaceae (*Callialasporites*), Taxodiaceae (*Inaperturopollenites*); and cool-type Taxodiaceae (*Concentrisporites*, *Exesipollenites*), Coniferophyta (*Pinaceae*, *Abietineaepollenites*, *Pinuspollenites*, *Cedripites*, *Parvisaccites*, *Piceaepollenites*, *Piceites*) [64–68,71]. In K_2n^{1+2}, the content of hot palynomorphs is 30.8%, the content of warm

palynomorphs is 28.2%, and the cool palynomorphs is 41%. In K_2s, the content of hot palynomorphs is 2.1%, the content of warm palynomorphs is 27.7%, and the cool palynomorphs is 70.2%. Summarizing, in the late Santonian–Campanian period, the vegetation generally showed that hot and warm types decreased from K_2n^{1+2} to K_2s, and the cool-type increased from K_2n^{1+2} to K_2s, indicating that the temperature decreased from late Santonian to early Campanian K_2n^{1+2} to late Campanian K_2s (Table 3).

Table 3. Climate-types table.

Palynomorphs	Climate type	References
Classopollis	Hot Type	[60,64–74]
Foraminisporis	Warm Type	
Osmundacidites	Warm Type	
Callialasporites	Warm Type	
Inaperturopollenites	Warm Type	
Concentrisporites	Cool Type	
Exesipollenites	Cool Type	
Pinaceae	Cool Type	
Abietineaepollenites	Cool Type	
Pinuspollenites	Cool Type	
Cedripites	Cool Type	
Parvisaccites	Cool Type	
Piceaepollenites	Cool Type	
Piceites	Cool Type	

The change in Santonian to Campanian temperature in the Songliao Basin is supported by the palynomorphs and plants in Jiayin Basin, which is located northeast of the Songliao Basin [62]. The Santonian flora of the Jiayin Basin indicate relatively hot to warm climate, while the late Campanian to Maastrichtian flora of the Jiayin Basin imply a relatively cool climate [62,75]. The paleoclimate of the Jiayin Basin is consistent with the overall climate-change response revealed in borehole ZKY2-1 in the late Santonian to Campanian period, suggesting that palynomorphs of borehole ZKY2-1 indicate adaptation to the climate during the late Santonian–Campanian period. According to oxygen isotope and TEX86 recorded in marine sediments, the global temperature decreased from late Santonian to late Campanian [1,7,76–79], which is also consistent with the palynological analysis of ZKY2-1. In combination with the dryness and humidity, that is, from the late Santonian to late Campanian period, the overall climate changed from a semiarid–semihumid warm climate to a semiarid–semihumid cool climate (Figure 9).

A series of evidence confirmed a decline in global temperature [1,7] and rapid radiation of angiosperm pollen [38,80] during the Late Cretaceous. However, there are few studies on the relationship between global temperature decline and angiosperm pollen evolution during the Late Cretaceous. This study on borehole ZKY2-1 clearly shows that the decline of global temperature during the Santonian–Campanian may have promoted the rapid radiation of angiosperm pollen. Because angiosperm pollen could adapt to more complex environments, including changeable or cold temperatures, the cooling during the late Campanian period may have been conducive to the adaptation and radiation of angiosperm pollen, and the second is not conducive to the prosperity of ferns spores and gymnosperm pollen, which objectively further promotes the further radiation of angiosperm pollen. Nevertheless, this study only puts forward a preliminary hypothesis and the relationship between the two needs further in-depth study.

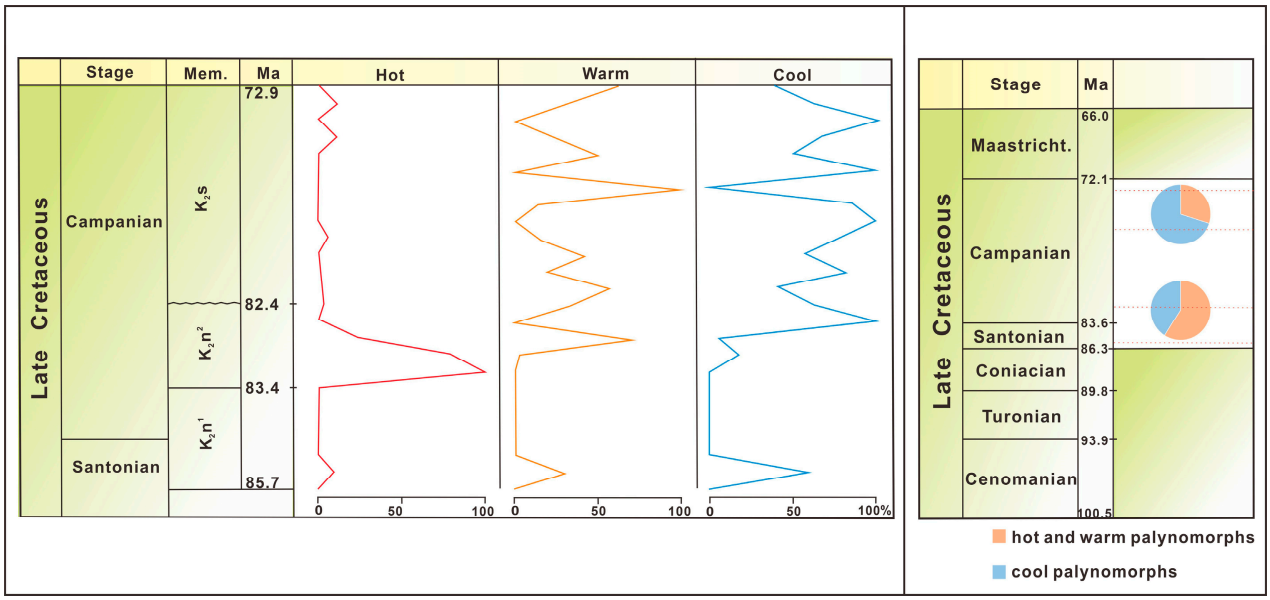

Figure 9. Percentage distribution map of typical thermally adaptable species in borehole ZKY2-1 and a pie chart of typical temperature changes for the Santonian–Campanian stage.

6. Conclusions

Palynomorphs are abundant in the Late Cretaceous stratigraphy in the Songliao Basin, indicative of climate change and vegetation evolution. Borehole ZKY2-1 provides valuable materials for studying palynomorphs in the Songliao Basin. Borehole ZKY2-1 can be well correlated with borehole SK1, with K_2n^1 dated as late Santonian, K_2n^2 determined as the latest Santonian–earliest Campanian, and K_2s assigned as late Campanian.

From late Santonian–earliest Campanian to late Campanian, the vegetation type of NE Asia changed from coniferous forest and herb to herb and broadleaf mixed forest. In addition, angiosperm pollen was radiated rapidly from late Santonian to late Campanian.

Although humidity was relatively stable, with semiarid to semihumid climate during the late Santonian to Campanian period, the temperature changed from a warm climate during the late Santonian–earliest Campanian to a cool climate during the late Campanian. The decline of global temperature may have promoted the evolution and expansion of angiosperm pollen.

Author Contributions: Conceptualization, D.X.; methodology, Z.Z., W.Y., J.Z. and X.M.; resources, D.X., Y.Y. and L.S.; data curation, D.X. and Z.Z.; writing—original draft preparation, Z.Z. and D.X.; writing—review and editing, D.X. and Z.Z.; supervision, D.X.; project administration, D.X.; funding acquisition, D.X. and X.W. All authors have read and agreed to the published version of the manuscript.

Funding: This research was supported by the National Key R&D Program of China (grant no. 2019YFC0605403, 2022YFF0800802), the National Natural Science Foundation of China (42288201, 41790452), and the Chinese "111" Project (B20011). This is a contribution to UNESCO/IUGS IGCP project 679, "Cretaceous Earth Dynamics and Climate in Asia."

Acknowledgments: We sincerely thank Shi Dunjiu from the Experimental Institute of Liaohe Exploration and Development Research Institute for his guidance and help. Thanks to Dai Wenyao, Majid Khan, and Ning Yafeng for their help in the laboratory work.

Conflicts of Interest: The authors declare no conflict of interest.

References

1. O'Brien, C.L.; Robinson, S.A.; Pancost, R.D.; Sinninghe Damsté, J.S.; Schouten, S.; Lunt, D.J.; Alsenz, H.; Bornemann, A.; Bottini, C.; Brassell, S.C.; et al. Cretaceous sea-surface temperature evolution: Constraints from TEX86 and planktonic foraminiferal oxygen isotopes. *Earth Sci. Rev.* **2017**, *172*, 224–247. [CrossRef]
2. Haq, B.U. Cretaceous eustasy revisited. Glob. *Planet Chang.* **2014**, *113*, 44–58. [CrossRef]
3. Hay, W.W. Toward understanding Cretaceous climate–An updated review. *Sci. China Earth Sci.* **2017**, *60*, 5–19. [CrossRef]
4. Jenkyns, H.C. Geochemistry of oceanic anoxic events. *Geochem. Geophys. Geosyst.* **2010**, *11*, 3. [CrossRef]
5. Sames, B.; Wagreich, M.; Wendler, J.E.; Haq, B.U.; Conrad, C.P.; Melinte-Dobrinescu, M.C.; Hu, X.; Wendler, I.; Wolfgring, E.; Yilmaz, I.Ö.; et al. Review: Short-term sea–level changes in a greenhouse world–A view from the Cretaceous. *Palaeogeogr. Palaeoclimatol. Palaeoecol.* **2016**, *441*, 393–411. [CrossRef]
6. Luft-Souza, F.; Fauth, G.; Bruno, M.D.R.; De Lira Mota, M.A.; Vázquez-García, B.; Santos Filho, M.A.B.; Terra, G.J.S. Sergipe–Alagoas Basin, Northeast Brazil: A reference basin for studies on the early history of the South Atlantic Ocean. *Earth Sci. Rev.* **2022**, *229*, 104034. [CrossRef]
7. Huber, B.T.; MacLeod, K.G.; Watkins, D.K.; Coffin, M.F. The rise and fall of the Cretaceous Hot Greenhouse climate. *Glob. Planet. Chang.* **2018**, *167*, 1–23. [CrossRef]
8. Petrizzo, M.R.; MacLeod, K.G.; Watkins, D.K.; Wolfgring, E.; Huber, B.T. Late Cretaceous paleoceanographic evolution and the onset of cooling in the Santonian at southern high latitudes (IODP site U1513, SE Indian Ocean). *Paleoceanogr. Paleoclimatol.* **2022**, *37*, e2021PA004353. [CrossRef]
9. Forster, A.; Schouten, S.; Moriya, K.; Wilson, P.A.; Sinninghe Damsté, J.S. Tropical warming and intermittent cooling during the Cenomanian/Turonian Oceanic Anoxic Event 2: Sea surface temperature records from the equatorial Atlantic. *Paleoceanography* **2007**, *22*. [CrossRef]
10. Van Helmond, N.A.; Sluijs, A.; Reichart, G.J.; Sinninghe Damsté, J.S.; Slomp, C.P.; Brinkhuis, H. A perturbed hydrological cycle during Oceanic Anoxic Event. *Geology* **2014**, *42*, 123–126. [CrossRef]
11. Zhang, L.M.; Wang, C.S.; Wignall, P.B.; Kluge, T.; Wan, X.; Wang, Q.; Gao, Y. Deccan volcanism caused coupled pCO2 and terrestrial temperature rises, and pre-impact extinctions in northern China. *Geology* **2018**, *46*, 271–274. [CrossRef]
12. Perez Loinaze, V.S.; Giordano, S.R.; Limarino, C.O. Late Cretaceous palynomorphs from the Golfo San Jorge Basin, Argentina. *J. S. Am. Earth Sci.* **2021**, *107*, 103151. [CrossRef]
13. Song, Z.C.; Shang, Y.K.; Liu, Z.S.; Huang, P.; Wang, X.F.; Qian, L.J.; Du, B.A.; Zhang, D.H. Palynology from China Volume II. In *Mesozoic Palynology*; Science Press: Beijing, China, 2000.
14. Heimhofer, U.; Hochuli, P.A.; Burla, S.; Oberli, F.; Adatte, T.; Dinis, J.L.; Weissert, H. Climate and vegetation history of western Portugal inferred from Albian near-shore deposits (Gale Formation, Lusitanian Basin). *Geol. Mag.* **2012**, *149*, 1046–1064. [CrossRef]
15. Li, J.G.; Batten, D.J.; Zhang, Y. Palynological record from a composite core through Late Cretaceous-Early Paleocene deposits in the Songliao Basin, Northeast China and its biostratigraphic implications. *Cretac. Res.* **2011**, *32*, 1–12. [CrossRef]
16. Zhang, M.Z.; Dai, S.; Heimhofer, U.; Wu, M.; Wang, Z.; Pan, B. Palynological records from two cores in the Gongpoquan Basin, central East Asia: Evidence for floristic and climatic change during the Late Jurassic to Early Cretaceous. *Rev. Palaeobot. Palynol.* **2014**, *204*, 1–17. [CrossRef]
17. Gao, R.Q.; Zhao, C.B.; Qiao, X.Y. *Palynology of Cretaceous Petroleum Strata in Songliao Basin*; The Geological Publishing House: Beijing, China, 1999.
18. Song, Z.C.; Zheng, Y.H.; Li, M.Y.; Zhang, Y.Y.; Wang, W.M.; Wang, D.N.; Zhao, C.B.; Zhou, S.F.; Zhu, Z.H.; Zhao, Y.N. *Palynology from China Vol. 1 Late Cretaceous and Tertiary Palynology*; Science Press: Beijing, China, 1999.
19. Zhang, M.Z.; Dai, S.; Ji, L.M.; Du, B.X.; Hu, S.S. Potential links between typical greenhouse climate of the Mid-Cretaceous and radiation evolution of early angiosperms. In Proceedings of the Abstracts of the 12th National Congress and 29th Annual Conference of the Paleontological Society of China, Zhengzhou, China, 17 September 2018; pp. 140–141.
20. Feng, Z.H.; Fang, W.; Wang, X.; Huang, C.Y.; Huo, Q.L.; Zhang, J.H.; Huang, Q.H.; Zhang, L. Micropaleontological and molecular fossil evidence for controlling oil shale formation by transgression in Songliao Basin. *Sci. China (Ser. D) Geosci.* **2009**, *39*, 1375–1386.
21. Wang, C.S.; Feng, Z.Q.; Zhang, L.M.; Huang, Y.; Cao, K.; Wang, P.; Zhao, B. Cretaceous paleogeography and paleoclimate and the setting of SKI borehole sites in Songliao Basin, northeast China. *Palaeogeogr. Palaeoclimatol. Palaeoecol.* **2013**, *385*, 17–30. [CrossRef]
22. Wan, X.Q.; Zhao, J.; Scott, R.W.; Wang, P.; Feng, Z.; Huang, Q.; Xi, D. Late Cretaceous stratigraphy, Songliao Basin, NE China: SK1 cores. *Palaeogeogr. Palaeoclimatol. Palaeoecol.* **2013**, *385*, 31–43. [CrossRef]
23. Xi, D.P.; Wan, X.Q.; Li, G.B.; Li, G. Integrated stratigraphy and time frame of the Cretaceous in China. *Chin. Sci. (Earth Sci.)* **2019**, *49*, 257–288.
24. Xi, D.P.; Li, S.; Jing, X.; Huang, Q.H.; Wang, C.; Si, W.M.; Wan, X.Q. Late Cretaceous paleoenvironment and paleoclimate change during large lake transgression in the Songliao Basin, NE China. *Earth Sci. Front.* **2009**, *16*, 123.
25. Jing, X. Late Cretaceous Palynological Fossil Assemblages and Their Paleoclimatic Records from Eastern Songliao Basin. Master's Thesis, China University of Geosciences, Beijing, China, 2011.
26. Zhao, J. Pollen, Algae and Paleoclimate and Paleoclimate Conditions of Early to Middle Cretaceous in Songliao Basin. Master's Thesis, China University of Geosciences, Beijing, China, 2013.
27. Ye, Y.Q. Classification and Biostratigraphic Correlation of Nonmarine Ostracods from the Late Cretaceous Nenjiang Formation to the Sifangtai Formation in Southwestern Songliao Basin. Master's Thesis, China University of Geosciences, Beijing, China, 2020.

28. Xi, D.P.; Wan, X.Q.; Feng, Z.Q.; Li, S.; Feng, Z.H.; Jian, J.Z.; Jing, X.; Si, W.M. The discovery of Late Cretaceous foraminifera from Songliao Basin: Evidence from the lake–sea communication of the SK–1 well. *Chin. Sci. Bull.* **2010**, *55*, 3433–3436.
29. Scott, R.W.; Wan, X.; Wang, C.; Huang, Q. Late Cretaceous chronostratigraphy (Turonian-Maastrichtian): SK1 core Songliao Basin, China. *Geosci. Front.* **2012**, *3*, 357–367. [CrossRef]
30. Xi, D.P.; Li, S.; Wan, X.; Jing, X.; Huang, Q.; Colin, J.; Wang, Z.; Si, W. Late Cretaceous biostratigraphy and paleoenvironmental reconstruction based on non-marine ostracodes nonmarine ostracodes from well SK1 (south), Songliao Basin, northeast China. *Hydrobiologia* **2012**, *688*, 113–123. [CrossRef]
31. Qu, H.; Xi, D.; Li, S.; Colin, J.P.; Huang, Q.; Wan, X. Late Cretaceous-Early Paleocene ostracod biostratigraphy of scientific drilling Sk1(N) in the Songliao Basin, northeast China. *J. Paleontol.* **2014**, *88*, 786–799. [CrossRef] [PubMed]
32. Zhao, J.; Wan, X.Q.; Xi, D.P.; Jing, X.; Li, W.; Huang, Q.H.; Zhang, J.Y. Late Cretaceouspalynology and paleoclimate change: Evidence from the SK1 (south) core, Songliao Basin, NE China. *Sci. China (Earth Sci.)* **2013**, *57*, 2985–2997. [CrossRef]
33. Ye, D.Q.; Huang, Q.H.; Zhang, Y. *Cretaceous Ostracod Biostratigraphy in Songliao Basin*; Petroleum Industry Press: Beijing, China, 2002.
34. Cheng, J.H.; He, C.C. Non-marine Cretaceous dinoflagellate biostratigraphy. Journal of stratigraphy. *J. Stratigr.* **2012**, *36*, 229–240.
35. Deng, C.L.; He, H.Y.; Pan, Y.X.; Zhu, R.X. Chronology of the terrestrial Upper Cretaceous in the Songliao Basin, northeast Asia. *Palaeogeogr. Palaeoclimatol. Palaeoecol.* **2013**, *385*, 44–54. [CrossRef]
36. Wu, H.C.; Zhang, S.H.; Jiang, G.Q.; Hinnov, L.; Yang, T.; Li, H.; Wan, X.; Wang, C. Astrochronology of the Early Turonian-Early Campanian terrestrial succession in the Songliao Basin, northeastern China and its implication for long-period behavior of the Solar System. *Palaeogeogr. Palaeoclimatol. Palaeoecol.* **2013**, *385*, 55–70. [CrossRef]
37. Wu, H.C.; Zhang, S.; Hinnov, L.A.; Jiang, G.; Yang, T.; Li, H.; Wan, X.; Wang, C. Cyclostratigraphy and orbital tuning of the terrestrial Upper Santonian-Lower Danian in Songliao Basin, northeastern China. *Earth Planet. Sci. Lett.* **2014**, *407*, 82–95. [CrossRef]
38. Ma, X.J.; Wu, H.C.; Fang, Q.; Shi, M.; Zhang, S.; Yang, T.; Li, H.; Wang, C. A floating astronomical time scale for the early Late Cretaceous continental strata in the Songliao Basin, Northeastern China. *Acta Geol. Sin. Engl. Ed.* **2020**, *94*, 27–37. [CrossRef]
39. Wang, T.T.; Wang, C.S.; Ramezani, J.; Wan, X.; Yu, Z.; Gao, Y.; He, H.; Wu, H. High-precision geochronology of the Early Cretaceous Yingcheng Formation and its stratigraphic implications for Songliao Basin, China. *Geosci. Front.* **2022**, *13*, 101386. [CrossRef]
40. Wang, P.J.; Xie, X.A.; Mattern, F.; Ren, Y.G.; Zhu, D.F.; Sun, X.M. The Cretaceous Songliao Basin: Volcanogenic succession, sedimentary sequence and tectonic evolution, NE China. *Acta Geol. Sin. (Engl.)* **2011**, *81*, 1002–1011.
41. Wang, Y.Q.; Sames, B.; Liao, H.Y.; Xi, D.; Pan, Y. Late Cretaceous ostracod fauna from the Shenjiatun section (Songliao Basin, Northeast China): Biostratigraphic and palaeoecological implications. *Cret. Res.* **2017**, *78*, 174–190. [CrossRef]
42. Yan, J.J.; Xi, D.P.; Yu, T.; Wan, X.Q. Biostratigraphy and environmental changes of the lower Nenjiang Formation in Qingshankou area, Songliao Basin. *J. Stratigr.* **2007**, *03*, 296–302.
43. Kohei, Y. Changes of Palynophytes During the Campanian to Maastricht (Late Cretaceous) in East Asia. Ph.D. Thesis, China University of Geosciences, Beijing, China, 2016.
44. Yu, Z.Q.; He, H.Y.; Deng, C.L.; Xi, D.; Qin, Z.; Wan, X.; Wang, C.; Zhu, R. New geochronological constraints for the Upper Cretaceous Nenjiang Formation in the Songliao Basin, NE China. *Cret. Res.* **2019**, *102*, 160–169. [CrossRef]
45. Cheng, Y.; Li, Y.; Wang, S.; Li, Y.; Ao, C.; Li, J.; Sun, L.; Li, H.; Zhang, T. Late Cretaceoust tectono–magmatic event in Songliao Basin, geochronology and geochemistry analysis, NE China: New Insights from mafic dyke geochronology and geochemistry analysis. *Geol. J.* **2018**, *53*, 2991–3008. [CrossRef]
46. Xie, X.; Yun, X.L. Three Cretaceous biota in Songliao Basin. In Proceedings of the China Conference, Guilin, China, 1 January 2013.
47. Kong, H.; Chen, C.R.; Dang, Y.M.; Yang, J.G.; Huang, Q.H.; Zhao, C.B. Review of three Cretaceous biota in Songliao Basin. *J. Paleontol.* **2006**, *45*, 416–424.
48. Huang, Q.H.; Chen, C.R.; Wang, P.Z.; Han, M.X.; Li, X.J.; Wu, D.Q. Late Cretaceous biological evolution and paleolake anoxic event in Songliao Basin. *Acta Micropalaeontol. Sin.* **1998**, *15*, 417–425.
49. Xi, D.P.; Wan, X.Q.; Feng, Z.Q.; Li, S.; Feng, Z.; Jia, J.; Jing, X.; Si, W. Discovery of Late Cretaceous foraminifera in the Songliao Basin: Evidence from SK-1 and implications for identifying seawater incursions. *Chin. Sci. Bull.* **2011**, *56*, 253–256. [CrossRef]
50. Gao, Y.F.; Wang, P.J.; Wang, C.S.; Ren, Y.G.; Wang, G.D.; Liu, W.Z.; Cheng, R.H. South Hole location, core profile characteristics and distribution of special lithologic layers of Songke 1 well. *Acta Geol. Sin.* **2008**, *5*, 669–675.
51. Feng, Z.Q.; Zhang, S.; Timothy, A.; Feng, Z.H.; Xie, X.N.; Zhao, B.; Fu, X.L.; Wang, C.S. Lacustrine turbidite channels and fans in the Mesozoic Songliao Basin, China. *Basin Res.* **2010**, *22*, 96–107. [CrossRef]
52. Cheng, R.H.; Wang, G.D.; Wang, P.J.; Gao, Y. Sedimentary microfacies and evolution of sedimentary environment of Sifangtai Formation and Mingshui Formation in the north hole of Songke 1 Well. *Earth Sci. Front.* **2009**, *16*, 85–95.
53. Wang, G.D.; Cheng, R.H.; Wang, P.J.; Gao, Y.F.; Wang, G.S.; Ren, Y.G.; Huang, Q.H. Fine description of the sedimentary sequence of the Upper Cretaceous Sifangtai Formation in the Songke 1 well in the Songliao Basin at centimeter scale: Lithology, lithofacies and cycle. *Earth Sci. Front.* **2011**, *18*, 263–284.
54. Nichols, D.J.; Sweet, A.R. *Biostratigraphy of Upper Cretaceous Nonmarine Palynofloras in a north-south Transect of the Western Interior Basin*; Geological Association of Canada–Special: Waterloo, ON, Canada, 1993; Volume 39, pp. 539–584.

55. Srivastava, S.K. Ephedralean pollen from the Upper Cretaceous Edmonton Formation of Alberta (Canada) and their paleoecological significance. *Can. J. Earth Sci.* **1968**, *5*, 211–221. [CrossRef]
56. Barrón, E.; Peyrot, D.; Rodríguez-Lopez, J.P.; Meléndez, N.; López del Valle, R.L.; Najarro, M.; Rosales, I.; Comas-Rengifo, M.J. Palynology of Aptian and Upper Albian (Lower Cretaceous) amber-bearing outcrops of the southern margin of the Basque-Cantabrian basin (northern Spain). *Cret. Res.* **2015**, *52*, 292–312. [CrossRef]
57. Nichols, D.J.; Jacobson, S.R. Cretaceous biostratigraphy in the Wyoming thrust belt. *Mt Geol.* **1982**, *19*, 73–78. [CrossRef]
58. Crane, P.R.; Friis, E.M.; Pedersen, K.R. The origin and early diversification of angiosperms. *Nature* **1995**, *374*, 27–33. [CrossRef]
59. Zhang, M.Z.; Ji, L.M.; Du, B.X.; Dai, S.; Hou, X. Palynology of the Early Cretaceous Hanxia Section in the Jiuquan Basin, Northwest China: The discovery of diverse early angiosperm pollen and paleoclimatic significance. *Palaeogeogr. Palaeoclimatol. Palaeoecol.* **2015**, *440*, 297–306. [CrossRef]
60. Wang, X. The dawn angiosperms: Uncovering the origin of flowering plants. *Lect. Notes Earth Sci.* **2010**, *121*, 1–4. [CrossRef]
61. Sauquet, H.; von Balthazar, M.; Magallón, S.; Doyle, J.A.; Endress, P.K.; Bailes, E.J.; Barroso de Morais, E.; Bull-Hereñu, K.; Carrive, L.; Chartier, M.; et al. The ancestral flower of angiosperms and its early diversification. *Nat. Commun.* **2017**, *8*, 16047. [CrossRef]
62. Sun, G.; Liang, F.; Yang, T.; Zhang, S.Q. *Late Cretaceous Flora from Jiayin of Heilongjiang*; Shanghai Science and Technology Press Education Press: Shanghai, China, 2020.
63. Sun, G.; Dong, Z.M.; Akhmetiev, M.; Markevich, V.; Godefroit, P.; Dlicher, D.L.; Sun, C.L.; Sun, Y.M.; Golovneva, L. *Late Cretaceous-Paleocene Biota and the K–Pg Boundary from Jiayin of Heilongjiang, China*; Shanghai Science, Technology and Education Publishing House: Shanghai, China, 2014; pp. 1–194.
64. Duan, Z.H. *Classopollis* and its paleoclimatic significance. *Coal Geol. Explor.* **1991**, *6*, 14–21.
65. Vakhrameev, V.A. Pollen Classopollis: Indicator of Jurassic and Cretaceous climate. *Palaeobotanists* **1981**, *28*, 301–307. [CrossRef]
66. Abbink, O.; Targarona, J.; Brinkhuis, H.; Visscher, H. Late Jurassic to earliest Cretaceous palaeoclimatic evolution of the southern North Sea. *Glob. Planet Chang.* **2001**, *30*, 231–256. [CrossRef]
67. Abbink, O.A.; van Konijnenburg-Van Cittert, J.H.A.; Visscher, H. A sporomorph ecogroup model for the northwest European Jurassic-Lower Cretaceous: Concepts and framework. *Neth. J. Geosci.* **2004**, *83*, 17–31. [CrossRef]
68. Deng, S.H. Paleoclimatic indicative significance of Mesozoic main plant fossils. *J. Palaeogeogr.* **2007**, *9*, 559–574.
69. Lin, M.Q. Late Jurassic to Early Cretaceous Palynological Flora in Northern China and Tibet and Its Paleoenvironmental Significance. Ph.D. Thesis, University of Science and Technology of China, Hefei, China, 2020.
70. Stukins, S.; Jolley, D.W.; McIlroy, D.; Hartley, A.J. Middle Jurassic vegetation dynamics from allochthonous palynological assemblages: An example from a marginal marine depositional setting; Lajas Formation, Neuquen Basin, Argentina. *Palaeogeogr. Palaeoclimatol. Palaeoecol.* **2013**, *392*, 117–127. [CrossRef]
71. Li, J.G.; Wu, Y.X.; Batten, D.J.; Lin, M. Vegetation and climate of the central and northern Qinghai-Xizang plateau from the Middle Jurassic to the end of the Paleogene inferred from palynology. *J. Asian Earth Sci.* **2019**, *175*, 35–48. [CrossRef]
72. Li, J.G.; Peng, J.G.; Zhang, Q.Q. Cretaceous sporopollen assemblages in the Gangbaqaqila section, Tibet. *J. Paleontol.* **2016**, *5*, 346–366.
73. Slater, S.M.; Twitchett, R.J.; Danise, S.; Vajda, V. Substantial vegetation response to Early Jurassic global warming with impacts on oceanic anoxia. *Nat. Geosci.* **2019**, *12*, 462–467. [CrossRef]
74. Gao, R.Q.; Zhang, Y.; Cui, T.C. *Cretaceous Petroleum Strata in Songliao Basin*; Petroleum Industry Press: Beijing, China, 1994.
75. Markevich, V.S.; Ashraf, A.R.; Bugdaeva, E.V. The Maastrichtian-Danian palynological assemblages from Wuyun of Jiayin nearby the Heilongjiang (Amur) River. In *Ancient Life and Modern Approaches; The 2nd International Congress of Paleontology*; IPC: Beijing, China, 2006; pp. 526–527.
76. Steinig, S.; Dummann, W.; Park, W.; Latif, M.; Kusch, S.; Hofmann, P.; Flögel, S. Evidence for a regional warm bias in the Early Cretaceous TEX86 record. *Earth Planet. Sci. Lett.* **2020**, *539*, 116184. [CrossRef]
77. Ji, L.M.; Zhang, M.Z.; Song, Z.G. The palynological record from Coniacian to Lower Campanian continental sequences in the Songliao Basin, northeastern China and its implications for palaeoclimate. *Cret. Res.* **2015**, *56*, 226–236. [CrossRef]
78. Wan, X.Q.; Wu, H.C.; Xi, D.P.; Liu, M.Y.; Qin, Z.H. Terrestrial biota and climate environment evolution during the Cretaceous Greenhouse Period in Northeast China. *Earth Sci. Front.* **2017**, *24*, 18–31. [CrossRef]
79. Keller, G. Cretaceous climate, volcanism, impacts, and biotic effects. *Cret. Res.* **2008**, *29*, 754–771. [CrossRef]
80. Coiffard, C.; Gomez, B. The rise to dominance of the angiosperm kingdom: Dispersal, habitat widening and evolution during the Late Cretaceous of Europe. *Lethaia* **2010**, *43*, 164–169. [CrossRef]